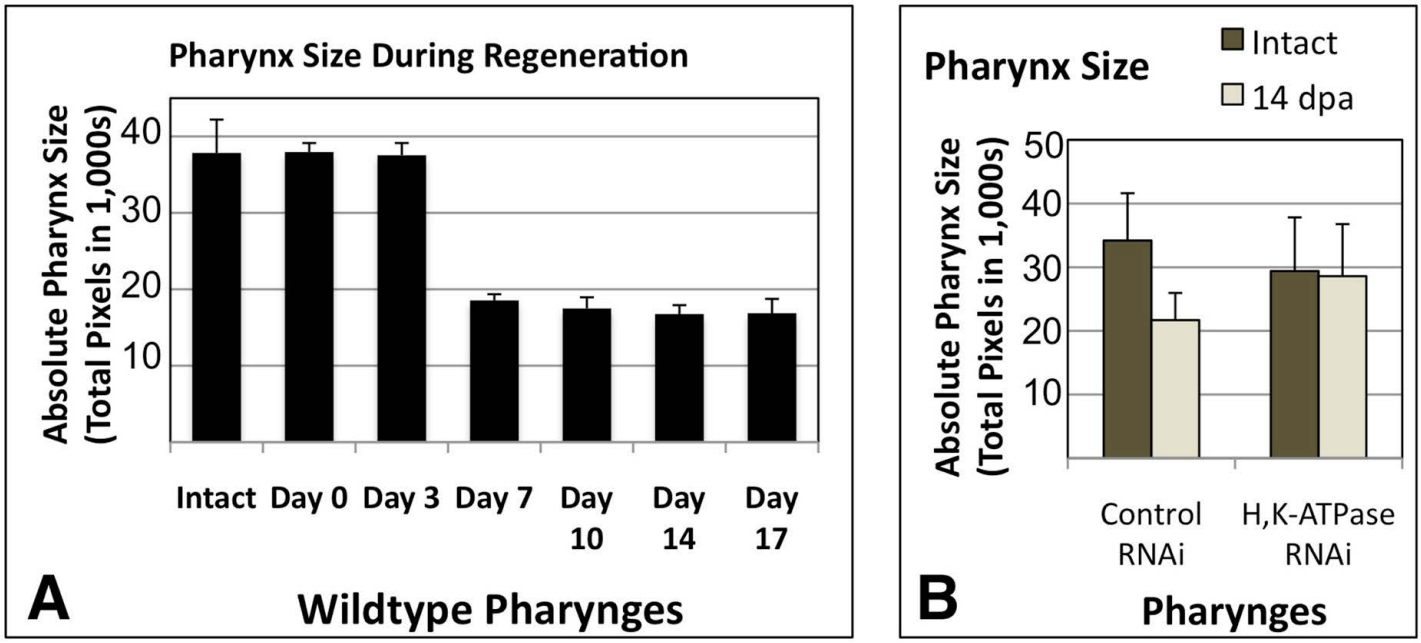

Fig. S1. Pharynx size decreases during regeneration in trunk fragments. Absolute numbers for pharynx area (given in pixels), as measured by morphology, of regenerating pharynx fragments (generated by cutting both above and below the pharynx of the original worm). (**A**) Pharynx size throughout regeneration in untreated controls in the same set of worms over 17 days. *n*=10 (except for intact, *n*=6). (**B**) Pharynx size of control RNAi versus H,K-ATPase RNAi regenerates in the same worms prior to amputation and on 14 dpa. *n*=15. Error bars: s.d.

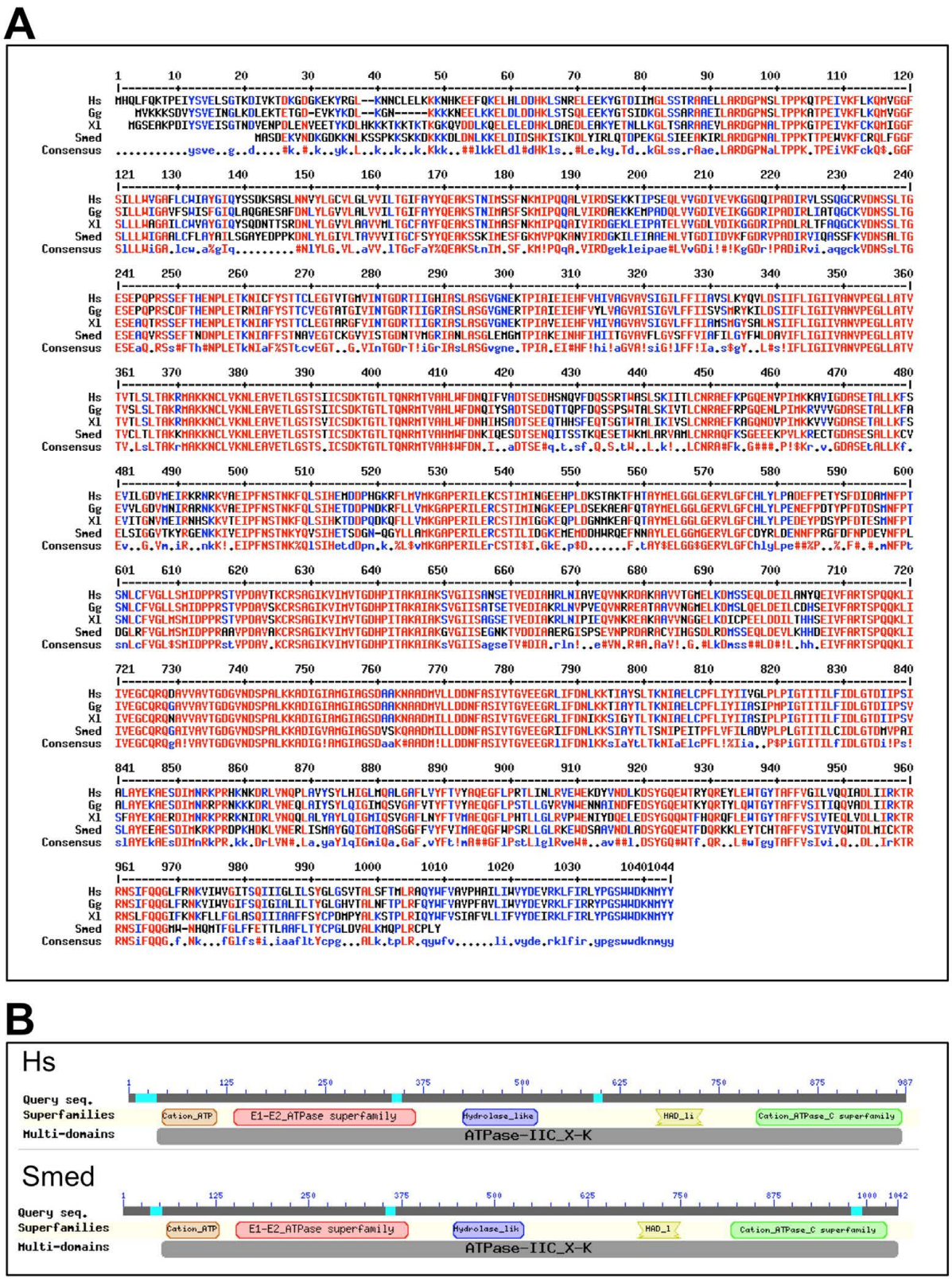

Fig. S2. Smed-H,K-ATPase is highly homologous to vertebrate non-gastric H,K-ATPase alpha subunits. (**A**) Alignment of Smed-H,K-ATPase protein sequences with other homologs: Hs, *Homo sapiens*; Gg, *Gallus gallus*; Xl, *Xenopus laevis*; Smed, *Schmidtea mediterranea*. Accession numbers: Hs-ATP12A (AAC37589.2), Gg-Potassium Transporting ATPase alpha chain 2 (NP_001026080.1), Xl-ATP12A (NP_001080818.1). Areas of high consensus (90%) in red; areas of low consensus (50%) in blue. (**B**) Alignment of Smed-H,K-ATPase and Hs-ATP12A protein domains.

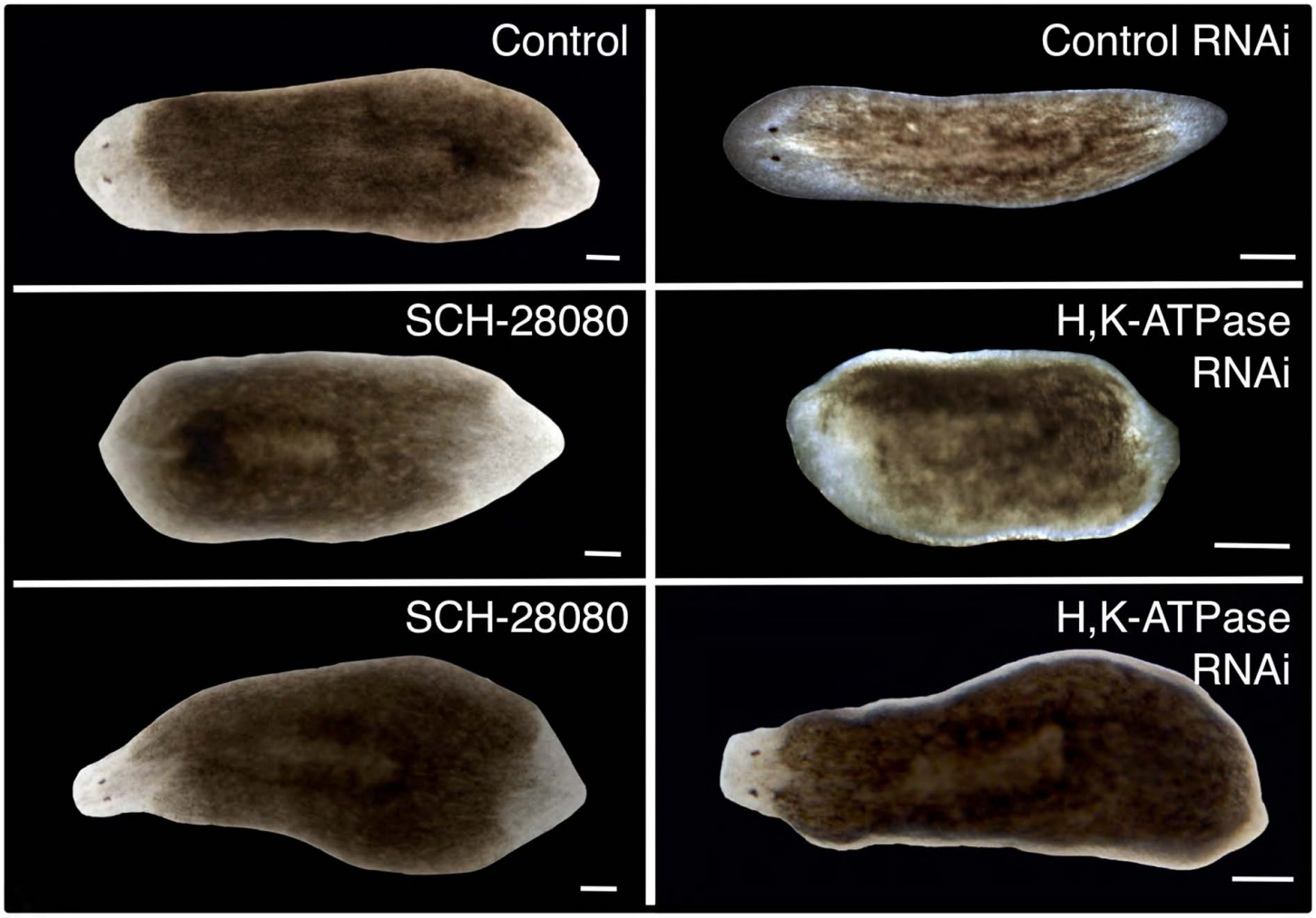

Fig. S3. H,K-ATPase activity is required for anterior blastema polarity and tissue remodeling in existing tissues. H,K-ATPase inhibition in *S. mediterranea* (14 dpa) by the highly specific inhibitor SCH-28080 and RNAi to the alpha subunit. H,K-ATPase inhibition was able to phenocopy the headless phenotype described in *D. japonica* (Beane et al., 2011). Both pharmacological and RNAi inhibition in *S. mediterranea* produced similar effects. SCH-28080: headless (6.1%), shrunken heads (35.1%), *n*=131. RNAi: headless (4.2%), shrunken heads (91.6%), *n*=166. Anterior left. Scale bars: 200 μm.

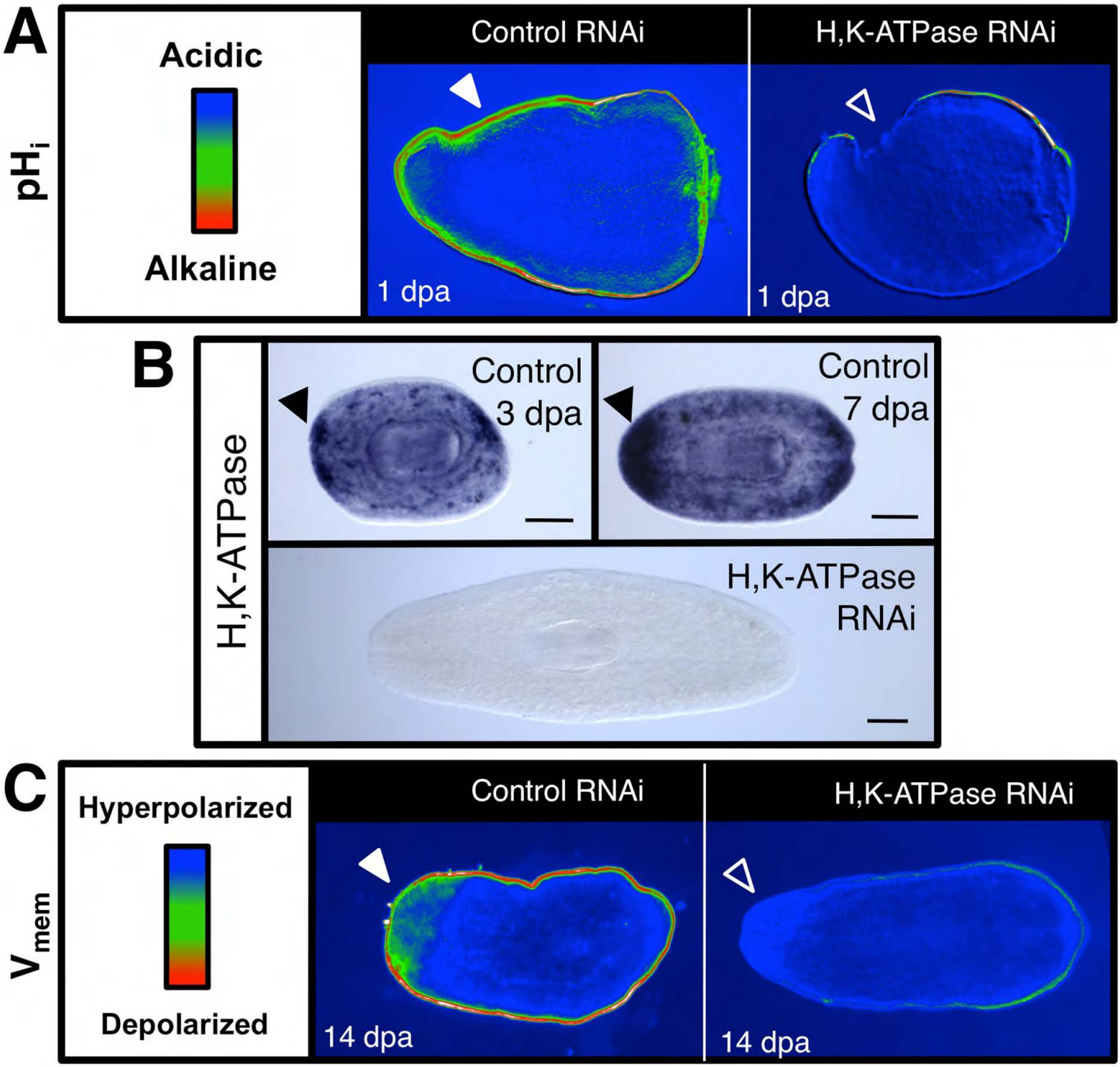

Fig. S4. H,K-ATPase inhibition results in membrane hyperpolarization and tissue acidification. (**A**) H,K-ATPase inhibition by RNAi in 24 hpa pharynx regenerates (anterior slant). pH_i reporter assay using SNARF-5F-AM. Red, relatively alkaline; blue, relatively acidic. Filled arrowheads denote presence and unfilled arrowheads absence of anterior alkalinization. Anterior is left. $n \geq 10$. (**B**) *In situ* hybridization showing *Smed-H,K-ATPase* expression in control (un-injected) pharynx regenerates and in an H,K-ATPase RNAi-injected intact worm. $n \geq 5$. Filled arrows indicate upregulated anterior expression. (**C**) H,K-ATPase inhibition by RNAi in 14 dpa pharynx regenerates. V_{mem} reporter assay using $DiBAC_4(3)$. Red, relatively depolarized; blue, relatively hyperpolarized. Filled arrowheads denote presence and unfilled arrowheads absence of anterior depolarization. Note that *Smed-H,K-ATPase(RNAi)* regenerates, although still strongly hyperpolarized compared with controls, have a slight but relatively more depolarized (lighter blue) anterior region corresponding to the area of the shrunken head. Anterior is left. $n \geq 8$.

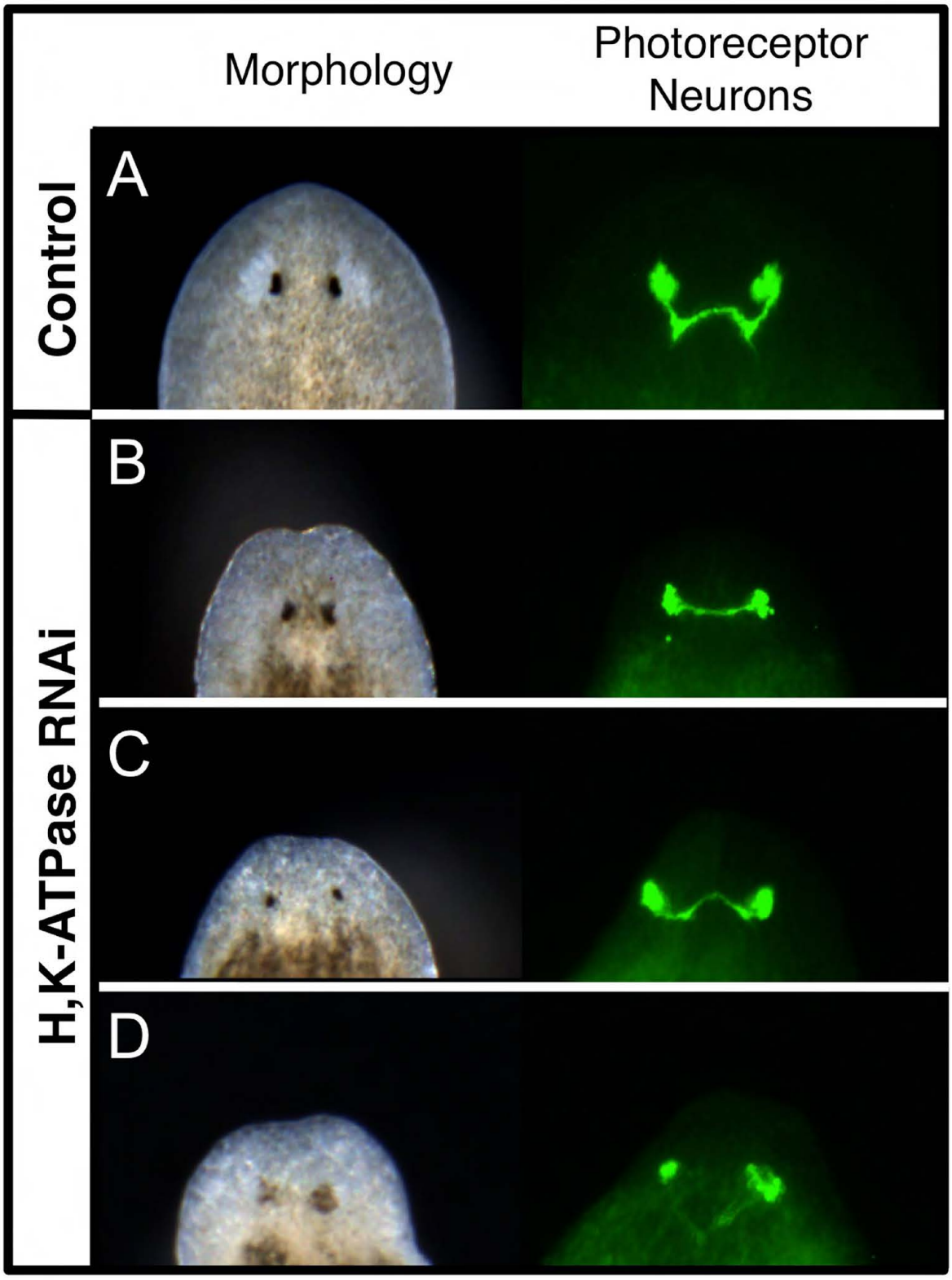

Fig. S5. H,K-ATPase inhibition affects eye innervation. (**A-D**) Eye regeneration in control (A) and H,K-ATPase-inhibited regenerates (B-D) at 14 dpa. Morphological views (dorsal) and photoreceptor neuron labeling (arrestin in green). H,K-ATPase-inhibited regenerates had severe innervation defects, many lacking an optic chiasm. Pigment cell regeneration was less affected, although some regenerates had smaller pigmented areas pigment (though still black, C) whereas others had light brown spots (indicative of reduced pigment production, D). All H,K-ATPase-inhibited animals lacked the white area which is normally visible in controls (surrounding the black pigment cells), suggesting that optic cup regeneration was abnormal in all regenerates. These data indicate that following H,K-ATPase inhibition, the neural defects resulting from the restriction of the head region lead to innervation and morphological defects in the eye.

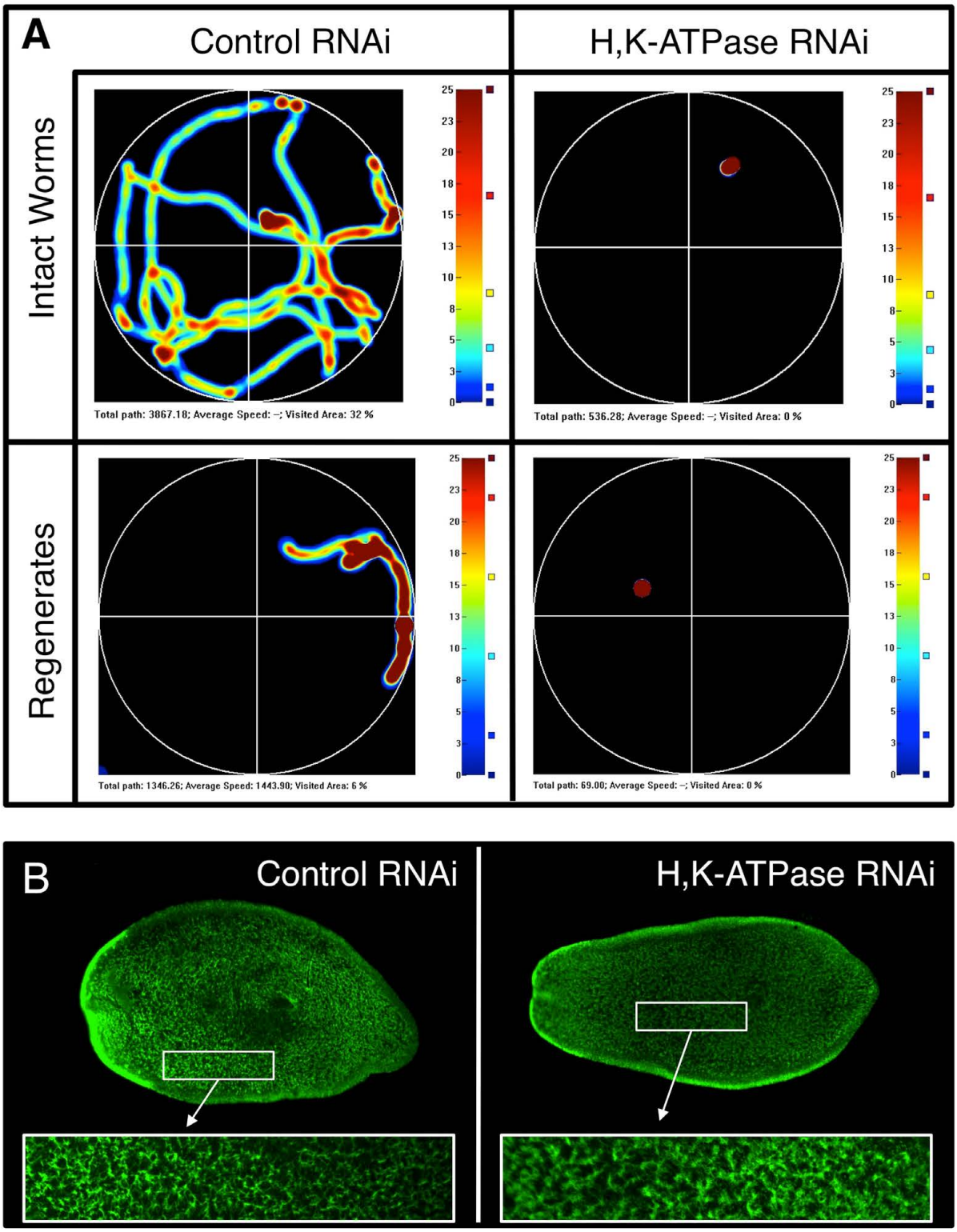

Fig. S6. H,K-ATPase inhibition results in locomotion defects without affecting the cilia used for movement. (**A**) Behavioral analyses of H,K-ATPase inhibited worms. Heat maps track movement of an individual worm over the span of 10 minutes. Red indicates most time spent in an area. Average area of dish covered in intact worms: 9.2% (control RNAi), 0.25% (H,K-ATPase RNAi), $n \geq 4$. Average area of dish covered in 14 dpa pharynx regenerates: 3.2% (control RNAi), 0% (H,K-ATPase RNAi), $n \geq 8$. Note that even intact, uncut H,K-ATPase RNAi-injected worms (at 2 weeks post injection) fail to exhibit exploratory behavior. (**B**) Anti-acetylated tubulin labeling of 14 dpa pharynx regenerates. Insets show higher magnification views of ventral cilia, present in both controls and H,K-ATPase RNAi-injected regenerates. $n \geq 6$.

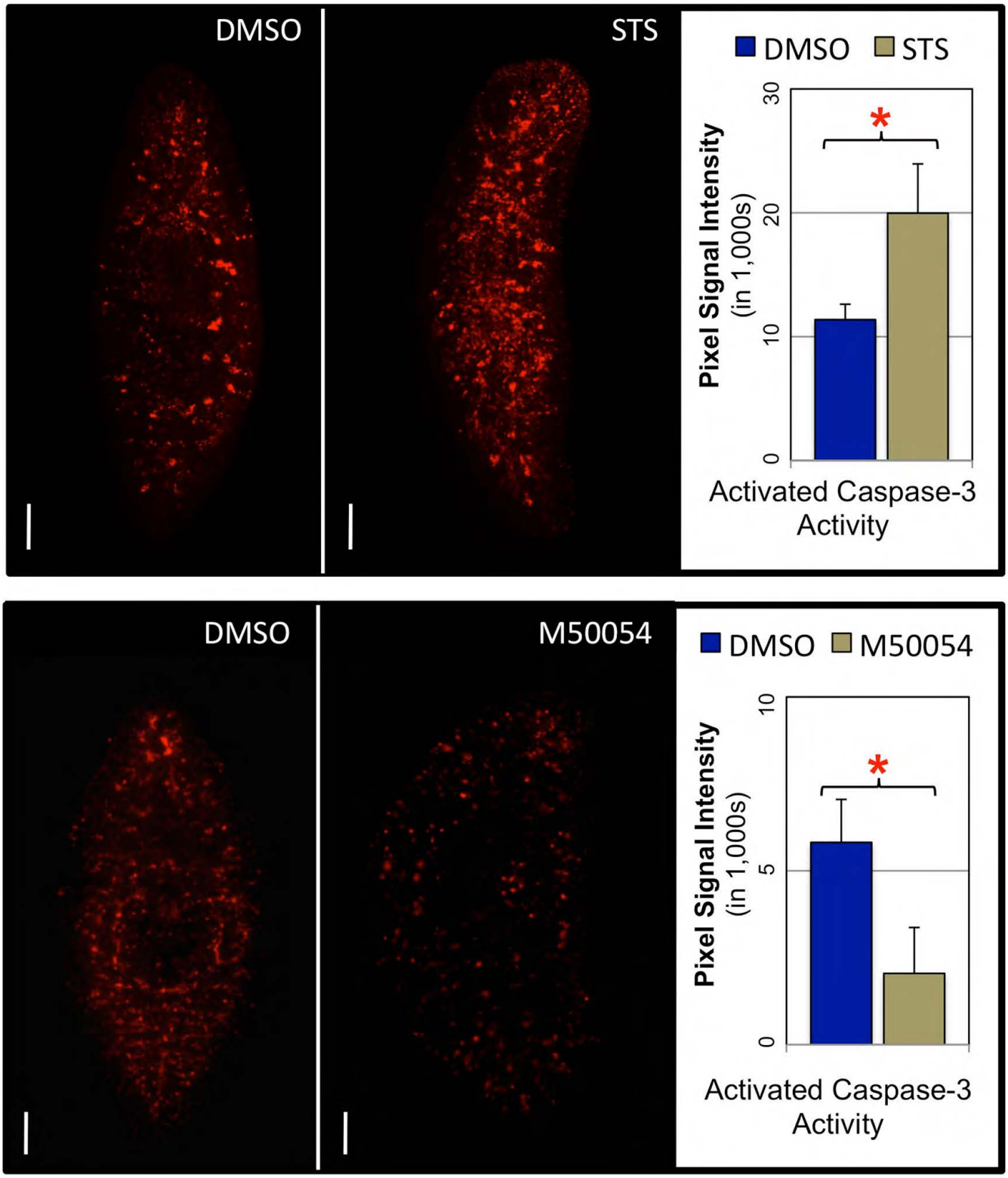

Fig. S7. Controls for anti-activated-caspase-3 labeling in planaria. (**A**) Labeling in control (DMSO) and staurosporine (STS, apoptotic inducer) treated intact worms. Animals treated for 6 hours (20 nM). (**B**) Labeling in control (DMSO) and M50054 (apoptotic inhibitor) treated intact worms. Animals treated for 4 days (100 μM). Anterior is up. Error bars: s.d. (n=5). *P<0.01. Scale bars: 200 μm.

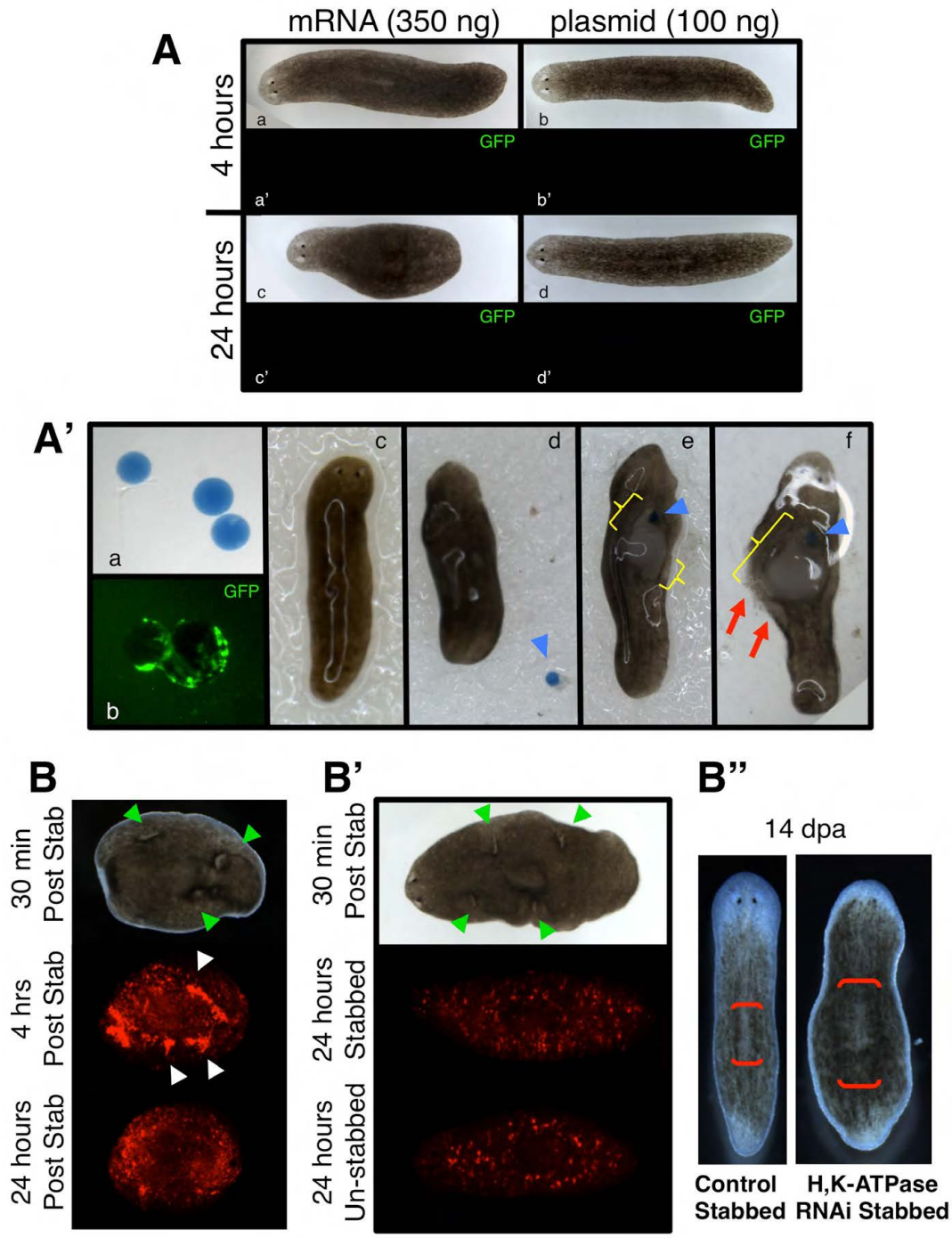

Fig. S8. Attempts to rescue H,K-ATPase by gain-of-function techniques or activation of apoptosis. (**A**,**A′**) Proof-of-principle assays for common gain-of-function techniques in planarians. (A) Whole planarians (*n*=10 each) injected with either GFP3 mRNA or pCS2-GFP3 plasmid failed to produce any GFP fluorescence at either 4 or 24 hours post injection. (A′) Micro-bead implantation in whole planarians. Roughly 80 μm diameter Affigel Blue beads (BioRad 153-7302, A2A) were coated with recombinant GFP protein (Vector Labs MB-0752, 1 mg/ml, A2B) using standard protocols. Worms were kept moist on a Kimwipe (A2C, dorsal), and placed ventral side up (A2D) prior to implantation. A small wound was created with #5 forceps, and a 'sticky' micro-bead with an attached small piece of Kimwipe (blue arrows) was placed into the wound (A2E). Worms immediately produced muscle contractions resulting in further wounds (yellow brackets). These began as small rips (A2E, brackets) but became progressively larger (A2F, bracket). All worms lysed (red arrows) and died by 30 minutes to 1 hour post implantation. (**B-B″**) Heated needle stab assay to rescue loss of H,K-ATPase by local activation of apoptosis (using 25 gauge steel needle). Brightfield and activated-caspase-3 staining shown. (B) Pharynx regenerates showing stabbing (green arrowheads) causes sites of upregulated apoptosis (white arrowheads) by 4 hours, but this upregulation is gone by 24 hours. (B′) Whole planarians showing that by 24 hours post stabbing (green arrowheads), there is no difference in apoptosis between stabbed and unstabbed animals. (B″) Control and H,K-ATPase RNAi pharynx regenerates showing that stabbing does not rescue the small head and overly large pharynx (red brackets) associated with loss of H,K-ATPase (*n*>18).